Annals of Pharmacology and Pharmaceutics

Review Article
Published: 23 Nov, 2016

Facile Synthesis of NaMN, NaAD and Derivatives

*Marci Wood and Yana Cen**

Department of Pharmaceutical Sciences, Albany College of Pharmacy and Health Sciences, USA

Abstract

Simple and efficient syntheses of NAD^+, an important biological cofactor, and its precursors have been limited to amido versions. Here we report the novel synthesis of two previously overlooked NAD^+ precursors, NaMN and NaAD, using a common intermediate, *ethyl nicotinate riboside* (*O-ethyl-NaR*). In addition, these synthetic metabolites were shown to be substrates for NAD^+ biosynthetic enzymes and were sufficient to increase cellular NAD^+ levels.

Abbreviations

NAD^+: Nicotinamide Adenine Dinucleotide; NaAD: Nicotinic Acid Adenine Dinucleotide; NMN: Nicotinamide Mononucleotide; NaMN: Nicotinic Acid Mononucleotide; NR: Nicotinamide Riboside; NaR: Nicotinic Acid Riboside; NAM: Nicotinamide; NA: Nicotinic Acid; NAMPT: Nicotinamide Phosphoribosyltransferase; NMNAT: NMN Adenylyltransferase

Introduction

Interest in *nicotinamide adenine dinucleotide* (NAD^+) metabolism has steadily increased in the past few years with a rise in reviews focused on NAD^+ and enzymes involved in NAD^+ synthesis and consumption [1-4]. This comes as no surprise as NAD^+ is an essential cofactor involved in cellular redox chemistry, DNA repair and energy metabolism. One class of enzymes which consume NAD^+, the sirtuins, has been omnipresent in the recent literature and has renewed interest in NAD^+ precursors, including *nicotinic acid mononucleotide* (NaMN) and *nicotinic acid adenine dinucleotide* (NaAD). However, the lack of methodology in the synthesis of NaMN and NaAD has impaired any further studies.

The intracellular NAD^+ level is maintained through the coordinated control of complementary *de novo* and salvage pathways. The *de novo* pathway begins with dietary tryptophan in eukaryotes and aspartate in microbes, and after a number of enzymatic steps results in the formation of an important precursor, NaMN [5]. The salvage pathway involves either *nicotinic acid* (NA) or *nicotinamide* (NAM). In microbes, NAM is converted to NA by the enzyme *nicotinamidase*, which then enters the Preiss-Handler pathway [6-9]. In contrast, mammals lack *nicotinamidase* and the salvage pathway utilizes NAM directly to form *nicotinamide* adenine mononucleotide (NMN) using the enzyme *nicotinamide phosphoribosyltransferase* (NAMPT) [10].

Interestingly, in the majority of microbes, the *de novo* and salvage pathways converge on a common intermediate, NaMN and must proceed through another intermediate, NaAD, to form NAD^+. Because of this convergence, both enzymes involved in the final two steps of NAD^+ formation, *NMN adenylyltransferase* (NMNAT) and NAD^+ synthetase, have been identified as suitable drug targets, namely against microbial infections [11,12]. This has increased the need for a simple and flexible synthetic scheme for NAD^+ precursors using a common intermediate to allow for divergent downstream synthesis.

In order to fully understand the roles of NaMN and NaAD in cellular metabolism, we sought to chemically synthesize NaMN and NaAD. However, the current literature for synthesis of NAD^+ precursors is limited to synthetic methods which only form the amido versions or those unsuitable for downstream 5'-OH phosphorylation. [13-15]. In fact, there are no reported syntheses of NaMN or NaAD and as of yet, the commercial supplies of both compounds have been erratic or unavailable. This increases the need for a complete and efficient synthesis of NaMN and NaAD. We report herein the chemical synthesis of NaMN and NaAD along with a number of ester precursors and derivatives.

Synthesizing NaMN and NaAD directly from *nicotinic acid riboside* (NaR) presents a number of difficulties. The acid moiety, as compared to the amide, is very reactive and highly charged. In

OPEN ACCESS

Correspondence:
Yana Cen, Department of Pharmaceutical Sciences, Albany College of Pharmacy and Health Sciences, 261 Mountain View Drive, Colchester, VT 05446, USA, Tel: 802-735-2647;
E-mail: Yana.Cen@acphs.edu

Received Date: *23 Oct 2016*
Accepted Date: *16 Nov 2016*
Published Date: *25 Nov 2016*

Citation:
Wood M, Cen Y. Facile Synthesis of NaMN, NaAD and Derivatives. Ann Pharmacol Pharm. 2016; 1(2): 1007.

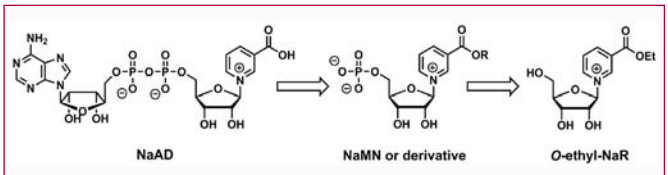

Scheme 1: Retrosynthetic analysis for NaMN and NaAD.

order to form the mononucleotide synthetically, the 5'-OH must be selectively phosphorylated without disturbing the acid group. One study attempted to use a silyl group to protect the acid, however, this protecting group proved to be unstable in the ribose-coupling reaction. [14]. For the synthesis of NaMN and NaAD, we made use of an prior observation that different *O*-ester derivatives of NaR spontaneously decompose to NaR under mild aqueous conditions. These *O*-esters were found to be stable during phosphorylation and adenylation but were labile enough to be readily hydrolyzed at the culmination of the synthesis. With this concept in mind, we proposed to phosphorylate *O*-ester derivative of NaR directly to form the mononucleotide, which could then be adenylated into the dinucleotide (Scheme 1).

Elevated intracellular NAD^+ concentration has been shown to provide protective effects against a broad spectrum of pathological conditions including neurodegeneration [16-18] diabetes, [19,20] obesity [21], hearing loss [22], and liver cancer [23]. A recent study also suggested that repletion of NAD^+ could extend the life span in mice. [24]. Previous studies have demonstrated the ability of NR, NaR, *O-methyl-NaR*, and *O-ethyl-NaR* to increase cellular NAD^+ levels [25]. The effect of the *O-ester mononucleotides* on overall NAD^+ levels has not been examined. The presence of the ester functionality could potentially increase the bioavailability of these compounds. With the synthetic NAD^+ precursors in hand, we further investigated the effect of the *O-ester mononucleotides* on cellular NAD^+ concentrations.

Methods and Materials

Reagents and instrument

All reagents were purchased from Aldrich or Fisher Scientific and were of the highest purity commercially available. UV spectra were obtained with a Varian Cary 300 Bio UV-visible spectrophotometer. HPLC was performed on a Dionex Ultimate 3000 HPLC system equipped with a diode array detector using Macherey-Nagel C18 reverse-phase column. NMR spectra were acquired on a Bruker AVANCE III 500 MHz high-field NMR spectrometer and the data was processed using Topspin software. HRMS was acquired with either a Waters micromass Q-tof Ultima or a Thermoscienctific Q-Exactive hybrid Quadrupole Orbitrap.

Synthesis of *Ethyl nicotinate riboside (O-ethyl-NaR)* (1): *Ethyl nicotinate riboside* was synthesized as previously described [25].

Synthesis of *Ethyl nicotinate mononucleotide (O-ethyl-NaMN):* (2): To a flame dried round-bottom flask were added *ethyl nicotinate riboside* (213 mg, 0.75 mmol) and 1 mL of *trimethylphosphate*. At 0°C, *phosphorus oxychloride* (1.68 g, 11 mmol) was added drop wise to the reaction mixture. The solution was stirred at 0°C for 3 hr. Ice was added to quench the reaction, and the pH was adjusted to 7 by addition of *ammonium hydroxide*. The crude product was concentrated and purified on a C18 reverse phase column using water as the eluent. The fractions containing desired product were combined and lyophilized to dryness to afford *ethyl nicotinate mononucleotide* (164 mg, 0.45 mmol, 60%) as a yellowish syrup. ^{1}H NMR (D_2O, 500 MHz) (ppm): 1.42 (t, *J*= 7.1 Hz: 3H), 4.09 (m, 1H), 4.22 (m, 1H), 4.46 (m, 1H), 4.55 (m, 2H), 4.59 (stack, 2H), 6.22 (d, *J*= 4.8 Hz, 1H), 8.36 (t, J= 6.6 Hz, 1H), 9.12 (d, J= 8 Hz, 1H): 9.53 (s, 1H). HRMS (M^+): calculated for $C_{13}H_{19}NO_9P^+$: 364.0792; found: 364.0783.

Synthesis of *Nicotinic acid mononucleotide* (NaMN): (2a): *Ethyl nicotinate mononucleotide* (5 mg, 0.014 mmol) was dissolved in 1 mL of 100 mM phosphate buffer pH 7.5, the reaction was incubated at 37°C for 16 hr. Reaction mixture was then concentrated and purified by C18 reverse phase column using water as the eluent. The fractions containing the desired product were combined and lyophilized to dryness to afford *nicotinic acid mononucleotide* (4.2 mg, 0.013 mmol, 89%) as a white solid. ^{1}H NMR (D_2O, 500 MHz) (ppm): 4.20 (m, 1H), 4.35 (m, 1H), 4.57 (t, J= 4.6 Hz, 1H), 4.74 (stack, 2H), 6.43 (d, J= 4.9 Hz, 1H), 8.47 (dd, J= 6.7, 7.8 Hz, 1H), 9.15 (d, J= 8.2 Hz, 1H), 9.44 (d, J= 6.3 Hz, 1H), 9.62 (s, 1H). HRMS (M^+): calculated for $C_{11}H_{15}NO_9P^+$: 336.0479; found: 336.0485.

Synthesis of *Nicotinic acid adenine dinucleotide* (NaAD): (3): A solution of *ethyl nicotinate mononucleotide* (80 mg, 0.22 mmol), *adenosine monophosphate* (AMP) (153 mg, 0.44 mmol) and $MgCl_2$ (502 mg, 5.28 mmol) in 5 mL of water was concentrated to dryness, 5 mL of 1.5 M HEPES-NaOH and 5 mL of 5 M EDCI were added to the residue to initiate the coupling reaction. Incubation for 16 hr at 37°C was followed by dilution with 3 mL of water. The reaction mixture was purified by C18 reverse phase chromatography using water as the eluent. The fractions containing the desired product were combined and lyophilized to dryness to afford *nicotinic acid adenine dinucleotide* (87 mg, 0.13 mmol, 59%) as a white solid. ^{1}H NMR (D_2O, 500 MHz) (ppm): 4.25 (stack, 3H), 4.38 (m, 1H), 4.44 (stack, 3H), 4.53 (stack, 2H), 4.75 (m, 1H), 6.07 (stack, 2H), 8.08 (t, J= 7.6 Hz, 1H), 8.18 (s, 1H), 8.46 (s, 1H), 8.76 (d, J= 8 Hz, 1H), 9.05 (d, J= 6.3 Hz, 1H), 9.15 (s, 1H). HRMS (M^+): calculated for $C_{21}H_{27}N_6O_{15}P_2^+$: 665.1004; found: 665.1018.

Stability of *Methyl nicotinate riboside* (*O-methyl-NaR*): A master-mix reaction containing 500 µM *O*-methyl-NaR in pH 7.5 *phosphate buffer* was incubated at 37°C. 30 µL of reaction was taken out at each time point and quenched with 3 µL of 10% TFA. Incubation time points include 0, 10, 20, 40: 60, 120, 240, and 360 minutes. The quenched reaction was then injected on a HPLC using a Macherey-Nagel Nucleosil C18 column with 20 mM *ammonium acetate* and 1:1 MeOH:H_2O isocratic system. Chromatograms were analyzed at 260 nm. Authentic chemical standard of NaR was injected to determine the retention time of product. Formation of NaR and consumption of *O-methyl-NaR* were quantitated by calculating the ratio between *O-methyl-NaR* and NaR area under each peak. A decomposition curve was generated using KaleidaGraph®.

Stability of *Ethyl nicotinate riboside* (*O-ethyl-NaR*): A master-mix reaction containing 500 µM *O*-ethyl-NaR in pH 7.5 phosphate buffer was incubated at 37°C. 30 µL of reaction was taken out at each time point and quenched with 3 µL of 10% TFA. Incubation time points include 0, 10, 20, 40, 60, 120, 240 and 360 minutes. The quenched reaction was then injected on a HPLC using a Macherey-Nagel Nucleosil C18 column with 20 mM ammonium acetate and 1:1 MeOH:H_2O isocratic system. Chromatograms were analyzed at 260 nm. Authentic chemical standard of NaR was injected to determine the retention time of product. Formation of NaR and consumption of *O*-ethyl-NaR were quantitated by calculating the ratio between *O-ethyl-NaR* and NaR area under each peak. A decomposition curve was generated using KaleidaGraph®.

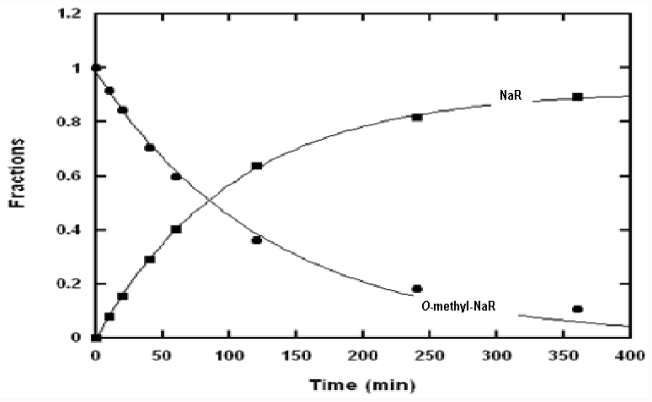

Figure 1: NaR formation from *O-methyl-NaR* hydrolysis. *O*-methyl NaR was incubated in 100 mM NH4OAc buffer pH 7.5 at 37 ˚C. 20 µL of reaction was aliquoted at each time point and quenched with 10% TFA. Incubation time points were 0, 10, 20, 40 60, 120, 240 and 360 minutes. The formation of NaR (solid rectangle) and hydrolysis of *O*-methyl-NaR (solid circle) were quantitated by HPLC. The ratio between O-methyl-NaR and NaR was determined for each time point. A half-life of 1 hour was determined from the curve-fit.

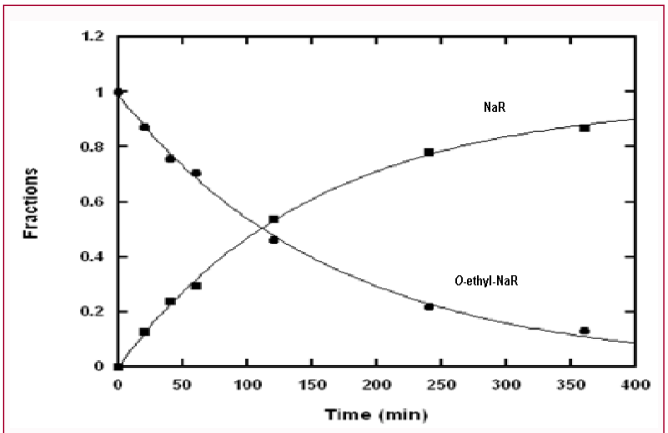

Figure 2: NaR formation from *O-ethyl-NaR* hydrolysis. *O-ethyl NaR* was incubated in 100 mM NH4OAc buffer pH 7.5 at 37˚C. 20 µL of reaction was aliquoted at each time point and quenched with 10% TFA. Incubation time points were 0, 10, 20, 40, 60, 120, 240 and 360 minutes. The formation of NaR (solid rectangle) and hydrolysis of *O-ethyl-NaR* (solid circle) were quantitated by HPLC. The ratio between *O-ethyl-NaR* and NaR was determined for each time point. A half-life of 2 hours was determined from the curve-fit.

Stability of *Ethyl nicotinate mononucleotide*: Reaction mixture of 270 μL containing 1 mM of ethyl nicotinate mononucleotide in 100 mM *phosphate buffer* pH 7.5 was incubated at 37˚C, aliquots (50 μL) from the reaction mixture was removed periodically over the next 16 hr and injected on HPLC for analysis. A Macherey-Nagel Nucleosil C18 column was employed with 20 mM *ammonium acetate* and 1:1 MeOH:H_2O isocratic system. Chromatograms were analyzed at 260 nm. Authentic chemical standard of *nicotinic acid mononucleotide* was injected to determine the retention time of product.

Expression and purification of yeast NMNAT

The gene *NMA1* was cloned from *Saccharomyces cerevisiae* gDNA into the protein expression vector, Pet28a (Novagen). The PetNMA1 vector was transfected into BL21-CodonPlus(DE3)-RIPL competent cells (Stratagene) and protein expression induced by 0.8 mM *isopropyl-β-D-thiogalactopyranoside* (IPTG) when the cells reached OD_{600} of 0.6~0.7 in LB media. The culture was grown for another at 37˚C before the cells were pelleted and lysed with 3 freeze-thaw cycles. The protein was purified using Ni-NTA resin (EMD Biosciences) affinity column and eluted with increasing concentrations of *imidazole*. The protein was aliquoted in 20% glycerol plus 2 mM DTT: flash frozen and stored at -80˚C. Protein concentration was determined using Bradford assay. The protein was >95% pure as determined by SDS-*polyacrylamide* gel electrophoresis.

Assay for NMNAT activity

A HPLC-based assay was used to test the activity of NMNAT. Reactions containing 500 µM synthetic NaMN, 2 mM ATP in 50 mM HEPES pH 7.6 with 20 mM $MgCl_2$ were initiated with the addition of 0.4 µM M NMNAT. The reactions were incubated at 37˚C for 2 or 20 minutes before being quenched with 10% TFA to pH 2. The samples were then injected on a HPLC fitted to a Macherey-Nagel Nucleosil C18 column. Substrates NaMN, ATP and product NaAD were resolved using a gradient of 0 to 10% methanol in 20 mM ammonium acetate. Chromatograms were analyzed at 260 nm. The peaks for NaMN and NaAD were compared to commercially available authentic standards.

Ethyl *nicotinate mononucleotide* serves as a substrate for NMNAT: Reactions containing 500 µM of ATP, 1 mM of *O*-ethyl-NaMN, 5 mM of $MgCl_2$ in 100 mM phosphate buffer pH 7.5 was initiated by addition of 1 unit of pyrophosphatase and 12.3 µM of NMNAT. For control experiment: 1 mM of NMN was used instead of *O-ethyl-NaMN*. The reactions were incubated at 37˚C for 16 hr and quenched by addition of 10% TFA to pH 2. After centrifugation at 14,500 rpm for 2 min, the samples were injected on a HPLC fitted to a Macherey-Nagel Nucleosil C18 column. Substrates and products were resolved using a gradient of 0 to 10% methanol in 20 mM ammonium acetate. Chromatograms were analyzed at 260 nm. Authentic ATP, NMN and NaAD were also injected for comparison.

Expression and purification of *S. pneumoniae* NAD^+ synthetase

The gene for NAD^+ Synthetase, *NadE*, was amplified from *Streptococcus pneumoniae* gDNA and cloned into the Pet28a vector (Novagen) at the NdeI-BamHI sites. The PetSPNadE vector was transfected into BL21-CodonPlus(DE3)-RIPL competent cells (Stratagene) and protein expression induced by 0.8 mM IPTG when the cells reached OD_{600} of 0.6~0.7 in LB media. The culture was grown for another hour at 37˚C before the cells were pelleted and lysed with 3 freeze-thaw cycles. The protein was purified using Ni-NTA resin (EMD Biosciences) affinity column and eluted with increasing concentrations of imidazole. The protein was aliquoted in 20% glycerol plus 2 mM DTT, flash frozen and stored at -80˚C. Protein concentration was determined using Bradford assay. The protein was >95% pure as determined by SDS-*polyacrylamide* gel electrophoresis.

Assay for NAD^+ synthetase activity

Reactions containing 50 µM synthetic NaAD, 100 µM ATP, 1 mM NH_4Cl in 25 mM HEPES, 500 µM $MgCl_2$, 50 mM KCl buffer, pH 8.0 were initiated with the addition of NAD^+ synthetase at 27 nM final concentration. The reactions were incubated at 25˚C for 4 or 60 min before being quenched with 10% TFA to pH 2. The samples were then injected on a HPLC fitted to a Macherey-Nagel Nucleosil C18 column. Substrates and product were resolved using a gradient of 0 to 10% *methanol* in 20 mM ammonium acetate. Chromatograms were analyzed at 260 nm. Authentic NaAD and NAD^+ samples were injected for comparison.

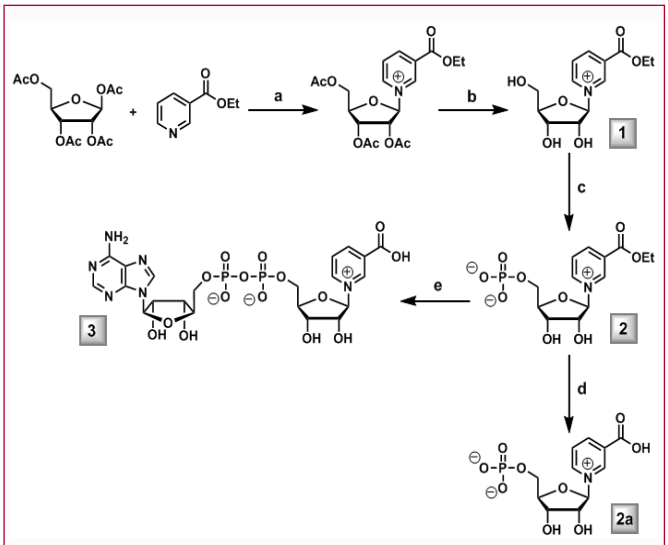

Scheme 2: Reagents: (a) TMSOTf, CH_2Cl_2, reflux; (b) NaOEt/EtOH: -20°C (80% yield for 2 steps); (c) $POCl_3$, trimethylphosphate (60% yield); (d) 100 mM phosphate buffer pH 7.5, 37°C (89% yield); (e) HEPES-NaOH, EDCI, AMP (59% yield).

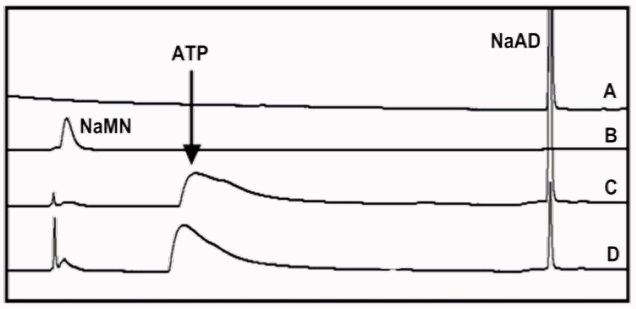

Figure 3: HPLC chromatograms showing that synthetic NaMN serves as a substrate for yeast NMNAT. (A) NaAD standard. (B) NaMN standard. (C) and (D) Enzymatic reactions of NaAD synthesis using synthetic NaMN as the substrate. The reactions contained 500 µM NaMN, 2 mM ATP, 20 mM $MgCl_2$ in 50 mM HEPES buffer pH 7.6. The reactions were initiated with the addition of 0.4 µM yeast NMNAT. They were incubated at 37°C for 2 min (D) or 30 min (C) before being quenched with 10% TFA. Reactions were then analyzed by HPLC assay as described in "Methods and Materials". After 2 min's incubation, the production of NaAD was already observed (D). After 30 min's incubation, almost all the NaMN was consumed (C).

Synthetic ethyl nicotinate mononucleotide increases intracellular NAD^+ level: HEK293 cells were plated onto 24-well plates and grown to 70~80% confluence. *Ethyl nicotinate mononucleotide* was added to the wells to achieve final concentrations of 0 µM, 500 µM, 750 µM, and 1 mM. The cells were incubated at 37°C for 12 hr. The cells were then pelleted and NAD^+ levels were measured using NAD^+ cycling assay as described previously [26]. For each sample, NAD^+ concentration was calculated in pmols per mg of protein where total protein concentration was determined by Bradford assay.

Results and Discussion

Several NR derivatives, including *O-methyl-NaR* and *O-ethyl-NaR*: have been shown to increase cellular NAD^+ concentrations [25]. Interestingly, *O-methyl-NaR* has been shown to be unstable in pH 7.5 buffer. With half-life of 1 hour, *O-methyl-NaR* spontaneously hydrolyzed to NaR as determined by HPLC assay (Figure 1). Since these NR derivatives are readily accessible, we further exploited the hydrolysis activity of *O-methyl-NaR* and *O-ethyl-NaR* for simple and efficient NaMN synthesis.

Similar to *O-methyl-NaR*, *O-ethyl-NaR* readily decomposed into NaR in mild aqueous conditions with a half-life of 2 hours (Figure 2). The decomposition in aqueous solution is unique to the nucleoside. In a related study, *O-ethyl nicotinate* was shown to be stable in 100 mM phosphate buffer pH 7.5 at 37°C as determined by ^1H NMR spectra. Only trace decomposition was detected when the temperature was raised to 60°C. The decomposition rate of *O*-ethyl-NaR at 37°C was 2-fold faster than that of *O-ethyl nicotinate* at 60°C (unpublished results). One possible explanation is that the partial positive charge on the pyridine in *O-ethyl-NaR* facilitates the subsequent ester hydrolysis. We chose *O-ethyl-NaR* as the precursor for NaMN synthesis for its easiness of production [25] and purification (Scheme 2). Furthermore, our preliminary study also indicated that the *O*-ester moiety was relatively stable under acidic condition, which should warranty the successful phosphorylation without disturbing the ester group. Indeed, after treatment with phosphorus oxychloride in trimethylphosphate, the desired mononucleotide, *O-ethyl-NaMN*, was obtained. This compound was purified by C18 reverse phase column chromatography. During purification, the byproducts can be easily separated from the desired product to provide pure *O-ethyl-NaMN* in decent yield (60% from O-ethyl-NaR). This intermediate was then directly hydrolyzed to NaMN. After 16 hr's incubation in 100 mM *phosphate buffer* pH 7.5 at 37°C, all the *O-ethyl-NaMN* was converted to NaMN. On the other hand, the complete synthesis of NaAD was accomplished by coupling *O-ethyl NaMN* and AMP in the presence of EDCI. The crude product, mostly *O-ethyl-NaAD*, was then purified on a C18 reverse phase column. Fractions containing the desired product were combined and lyophilized to dryness. The NMR spectrum of the lyophilized product showed a mixture of both

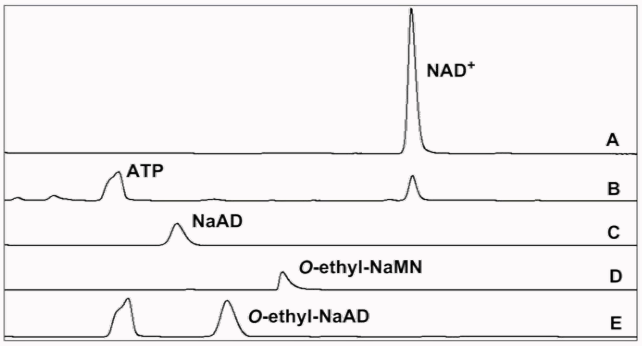

Figure 4: HPLC chromatograms showing that *O*-ethyl-NaMN serves as a substrate for yeast NMNAT. (A) NAD^+ standard. (B) Enzymatic synthesis of NAD^+ using yeast NMNAT. The reaction containing 1 mM NMN, 500 µM ATP, 5 mM $MgCl_2$ in 100 mM phosphate buffer pH 7.5 was initiated with the addition of 1 unit inorganic pyrophosphatase and 12.3 µM yeast NMNAT. The reaction was incubated at 37°C for 16 hr before being quenched with 10% TFA. The formation of NAD^+ indicated the recombinant enzyme was active, and this reaction served as the positive control for the following experiments. (C) NaAD standard. (D) *O*-ethyl-NaMN standard. (E) Enzymatic synthesis of *O*-ethyl-NaAD using *O*-ethyl-NaMN as the substrate. The reaction containing 1 mM *O*-ethyl-NaMN, 500 µM ATP, 5 mM $MgCl_2$ in 100 mM phosphate buffer pH7.5 was initiated with the addition of 1 unit inorganic pyrophosphatase and 12.3 µM yeast NMNAT. The reaction was incubated at 37°C for 16 hr before being quenched with 10% TFA. The reaction was then analyzed by HPLC assay as described in "Methods and Materials". The consumption of O-ethyl-NaMN led to the formation of a new compound which had similar retention time as NaAD standard. This compound was determined to be O-ethyl-NaAD by MS.

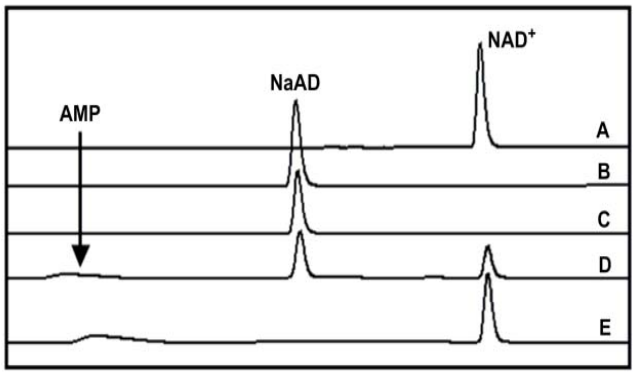

Figure 5: HPLC chromatograms showing that synthetic NaAD serves as a substrate for *S. pneumoniae* NAD^+ synthetase. (A) NAD^+ standard. (B) NaAD standard from the commercial source. (C) Synthetic NaAD. (D) and (E) Enzymatic synthesis of NAD^+ using synthetic NaAD as the substrate. Reactions containing 50 μM NaAD, 1 mM NH_4Cl, 500 μM $MgCl_2$, 50 mM KCl in 25 mM HEPES buffer pH8 were initiated with the addition of 27 nM of NAD synthetase. The reactions were incubated at 37°C for 4 min (D) or 60 min (E) before being quenched with 10% TFA. Reactions were then analyzed by HPLC assay as described in "Methods and Materials". After 4 min's incubation: the production of NAD^+ was observed (D). After 60 min's incubation, all the NaAD was converted to NAD^+ (E).

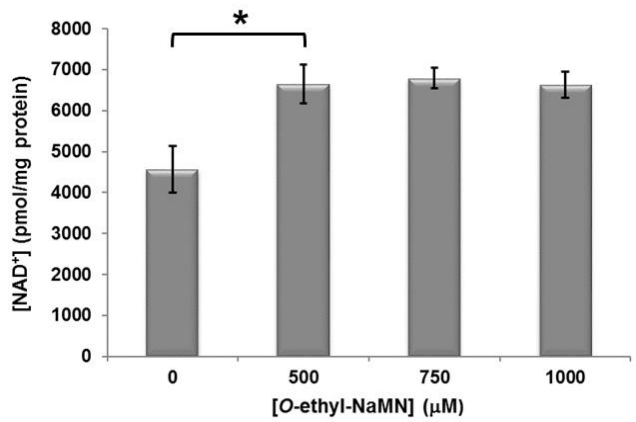

Figure 6: *O-ethyl-NaMN* increases intracellular NAD^+ concentration. HEK293 cells were treated with *O-ethyl-NaMN* to the final concentrations of 0 μM, 500 μM, 750 μM, and 1 mM. The cells were incubated at 37°C for 12 hr. The cells were then pelleted and NAD^+ levels were measured using NAD^+ cycling assay as described in "Methods and Materials". *O*-ethyl-NaMN was ableto increase the cellular NAD^+ up to 1.5-fold. $^*p < 0.05$.

O-ethyl-NaAD and NaAD, indicating that during purification and lyphilization *O-ethyl-NaAD* readily decomposed into NaAD. We took advantage of this observation and repeated the lyophilization procedure two more times to obtain pure NaAD in 59% yield. The synthetic NaMN and NaAD were fully characterized by NMR and high resolution mass spectrometry.

To further confirm the identity of these compounds, enzymatic synthesis of NaAD and NAD^+ were carried out using synthetic NaMN and NaAD, respectively. The synthetic NaMN was incubated with ATP in 50 mM HEPES pH 7.6 in the presence of 0.4 μM NMNAT. The reaction was allowed to react at 37°C before quenching. NaMN was readily converted by the yeast NMNAT enzyme as evidenced by the production of NaAD only after 2 min's incubation (Figure 3). NMNAT appears to tolerate the substitution at the acid functionality as *O-ethyl-NaMN* was also accepted as a substrate to form *O*-ethyl-NaAD (Figure 4). In this case, *O-ethyl-NaMN* was incubated with ATP in 100 mM phosphate buffer pH 7.5 with 12.3 μM NMNAT and 1 unit/reaction of inorganic *pyrophosphatase* at 37°C for 16 hr. The newly formed peak in the reaction mixture was concluded to be *O-ethyl-NaAD* as determined by LC/MS. A positive control reaction containing 1 mM NMN as substrate was carried out at the same time, and NAD^+ was the preferred product for NMNAT. The ability of NAD^+ synthetase from *S. pneumoniae* to use synthetic NaAD as a substrate was also investigated (Figure 5). Reactions containing NaAD, ATP and NH4Cl in 50 mM HEPES pH 8 were initiated with the addition of NAD^+ synthetase. After incubation at 25°C for merely 4 min: significant amount of NAD^+ was already being produced. These enzymatic syntheses not only prove the chemical identity of the synthetic compounds: but also open the possibility of generating novel NAD^+ derivatives using biosynthetic enzymes.

Recent studies suggested that intracellular NAD^+ level can be increased by both NR [21] and NMN [27]. But the effect of *O*-ester derivatives of NaMN on NAD^+ concentration remains elusive. We examined the effect of *O*-ethyl-NaMN on NAD^+ concentration in HEK293 cells. Cells were treated with various concentrations of synthetic *O*-ethyl-NaMN for 12 hr. NAD^+ concentrations were then measured as described before [26]. Treatment with 500 M *O*-ethyl-NaMN was able to elevate the cellular NAD^+ level by 1.5-fold (Figure 6). This increase seemed to plateau at 750 μM and 1 mM. In a previous study: NR demonstrated similar NAD^+ stimulating ability in HK293 cells [25] The current study suggested the cell permeability and bioactivity of *O*-ester derivatives of NaMN. We have successfully established a new and facile synthesis of the important NAD^+ precursors, NaMN and NaAD. The synthesis utilized a common precursor, *O-ethyl-NaR*. This compound can also be used for the divergent synthesis of other novel NAD^+ derivatives such as *O-ethyl-NaMN*. *O-ethyl-NaMN* not only serves as a substrate for yeast NMNAT in *in vitro* study, but also increases NAD^+ levels in HEK293 cells. The presence of ester functionality could potentially increase the bioavailability of this molecule as compared to the parent compound, NaMN. It has yet to be determined if *O-ethyl-NaMN* is a substrate for human NMNAT, but we have shown that this ester is readily hydrolyzed at neutral pH or by esterase to form NaMN, which could directly enter the NAD^+ biosynthetic pathway. Stable isotope labeled NAD^+ precursors can also be produced via this new synthetic methodology. Isotopically labeled precursors will facilitate the study of NAD^+ metabolism. In conclusion: this novel synthesis of NaMN, NaAD and derivatives will enable the further development and investigation of novel NAD^+ precursors.

Acknowledgement

This work was supported by start-up fund from Albany College of Pharmacy and Health Sciences (Y.C.). We would like to thank Dr. Lawrence C. Sowers at the University of Texas Medical Branch for the HRMS assistance.

References

1. Houtkooper RH, Cantó C, Wanders RJ, Auwerx J. The secret life of NAD^+: an old metabolite controlling new metabolic signaling pathways. Endocr Rev. 2010; 31: 194-223.
2. Magni G, Orsomando G, Raffelli N, Ruggieri S. Enzymology of mammalian NAD metabolism in health and disease. Front Biosci. 2008; 13: 6135-6154.
3. Yang Y, Sauve AA. NAD^+ metabolism: Bioenergetics: signaling and manipulation for therapy. Biochim Biophys Acta. 2016; 1864: 1787-1800.

4. Lin H. Nicotinamide adenine dinucleotide: beyond a redox coenzyme. Org Biomol Chem. 2007: 5: 2541-2554.

5. Bender: D. A. Biochemistry of tryptophan in health and disease. Mol Aspects Med. 1983; 6: 101-97.

6. Preiss J, Handler: P. Biosynthesis of diphosphopyridine nucleotide. I. Identification of intermediates. J Biol Chem. 1958; 233: 488-492.

7. Preiss J, Handler P. Biosynthesis of diphosphopyridine nucleotide II. Enzymatic aspects. The Journal of biological chemistry. 1958: 233: 493-500.

8. Frothingham R, Meeker-O'Connell WA, Talbot EA, George JW, Kreuzer KN. Identification: cloning: and expression of the Escherichia coli pyrazinamidase and nicotinamidase gene: pnc A. Antimicrob Agents Chemother. 1996; 40: 1426-1431.

9. Ghislain M, Talla E, François JM. Identification and functional analysis of the Saccharomyces cerevisiae nicotinamidase gene: PNC1. 2002: 19: 215-224.

10. Garten A, Petzold S, Körner A, Imai S, Kiess W. Nampt: linking NAD biology: metabolism and cancer. Trends Endocrinol Metab. 2009; 20: 130-138.

11. Magni G, Di Stefano M, Orsomando G, Raffaelli N, Ruggieri S. NAD(P) biosynthesis enzymes as potential targets for selective drug design. Curr Med Chem. 2009; 16: 1372-1390.

12. Gerdes SY, Scholle MD, D'Souza M, Bernal A, Baev MV, Farrell M, et al. From genetic footprinting to antimicrobial drug targets: examples in cofactor biosynthetic pathways. J Bacteriol. 2002; 184: 4555-4572.

13. Tanimori S, Ohta T, Kirihata M. An efficient chemical synthesis of nicotinamide riboside (NAR) and analogues. Bioorg Med Chem Lett. 2002; 12: 1135-1137.

14. Franchetti P, Pasqualini M, Petrelli R, Ricciutelli M, Vita P, Cappellacci L. Stereoselective synthesis of nicotinamide beta-riboside and nucleoside analogs. Bioorg Med Chem Lett. 2004; 14: 4655-4658.

15. Jaemoon Lee, Hywyn Churchil, Woo-Baeg Choi, Joseph E. Lynch, F. E. Roberts, R. P. Volante, et al. A chemical synthesis of nicotinamide adenine dinucleotide (NAD^+). Chemical Communications 1999: 729-730.

16. Qin W, Yang T, Ho L, Zhao Z, Wang J, Chen L, et al. Neuronal SIRT1 activation as a novel mechanism underlying the prevention of Alzheimer disease amyloid neuropathology by calorie restriction. J Biol Chem. 2006; 281: 21745-21754.

17. Sasaki Y, Araki T, Milbrandt J. Stimulation of nicotinamide adenine dinucleotide biosynthetic pathways delays axonal degeneration after axotomy. J Neurosci. 2006; 26: 8484-8491.

18. Gong B, Pan Y, Vempati P, Zhao W, Knable L, Ho L, et al. Nicotinamide riboside restores cognition through an upregulation of proliferator-activated receptor-gamma coactivator 1alpha regulated beta-secretase 1 degradation and mitochondrial gene expression in Alzheimer's mouse models. Neurobiol Aging. 201; 34: 1581-1588.

19. Samuel A.J. Trammell, Benjamin J. Weidemann, Ankita Chadda, Matthew S. Yorek, Amey Holmes, Lawrence J. Coppey, et al. Nicotinamide Riboside Opposes Type 2 Diabetes and Neuropathy in Mice. Scientific reports. 2016: 6: 26933.

20. Lee HJ, Hong YS, Jun W, Yang SJ. Nicotinamide Riboside Ameliorates Hepatic Metaflammation by Modulating NLRP3 Inflammasome in a Rodent Model of Type 2 Diabetes. J Med Food. 2015; 18: 1207-1213.

21. Cantó C, Houtkooper RH, Pirinen E, Youn DY, Oosterveer MH, Cen Y, et al. The NAD^+ precursor nicotinamide riboside enhances oxidative metabolism and protects against high-fat diet-induced obesity. Cell Metab. 2012; 15: 838-847.

22. Brown KD, Maqsood S, Huang JY, Pan Y, Harkcom W, Li W, et al. Activation of SIRT3 by the NAD^+ precursor nicotinamide riboside protects from noise-induced hearing loss. Cell Metab. 2014; 20: 1059-1068.

23. Djouder N. Boosting NAD^+ for the prevention and treatment of liver cancer. Mol Cell Oncol. 2015: 2: e1001199.

24. Zhang H, Ryu D, Wu Y, Gariani K, Wang X, Luan P, et al. NAD^+ repletion improves mitochondrial and stem cell function and enhances life span in mice. Science. 2016; 352: 1436-1443.

25. Yang T, Chan NY, Sauve AA. Syntheses of nicotinamide riboside and derivatives: effective agents for increasing nicotinamide adenine dinucleotide concentrations in mammalian cells. J Med Chem. 2007; 50: 6458-6461.

26. Fulco M, Cen Y, Zhao P, Hoffman EP, McBurney MW, Sauve AA, et al. Glucose restriction inhibits skeletal myoblast differentiation by activating SIRT1 through AMPK-mediated regulation of Nampt. Dev Cell. 2008; 14: 661-673.

27. Yoshino J, Mills KF, Yoon MJ, Imai S. Nicotinamide mononucleotide: a key NAD^+ intermediate: treats the pathophysiology of diet- and age-induced diabetes in mice. Cell Metab. 2011; 14: 528-536.